Ilorin Journal of Science
Volume 5, Number 2, 2018, pp. 79 – 91 (Printed in Nigeria)
ISSN: 2408 – 4840 © 2018 Faculty of Physical Sciences, University of Ilorin
https://doi.org/10.54908/iljs.2018.05.02.001

ILORIN
JOURNAL OF SCEINCE

ILJS-18-001

Mathematical Modeling of Transport Phenomena of Carbon Dioxide in Concrete Structures

Olayiwola[1]*, R. O., Cole[1], A. T., Adedayo[1], O. A. and Fenuga[2], O. J.

[1]Department of Mathematics, Federal University of Technology, Minna, Nigeria.
[2] Department of Mathematics, University of Lagos, Lagos, Nigeria.

Abstract

Concrete has a reputation as a "low tech" material, but it is actually very complex and worthy of study. It's the most widely used construction material in the world. Carbonation process in concrete regularly involves a chemical reaction between carbon dioxide (CO_2) and the products of cement hydration. By treating transport phenomena as a concrete carbonation process, this study presented a two-dimensional linear partial differential equation derived based on the principle of mass balance and convective-dispersive equation incorporating rate constant for zero-order production. We assume the diffusion coefficient of CO_2 in any direction of concrete is all the same. The analytical solution of the model is achieved by the eigenfunctions expansion technique. The results obtained are presented graphically and discussed. It is revealed that the relationships among CO_2 concentration, carbonation depth and time that can be used to state a carbonation transport phenomena in concrete structures are influenced by the diffusion coefficient.

Keyword: carbonation, carbon dioxide, cement, concrete structures, eigenfuction expansion technique.

1. Introduction

The cement manufacturing process has been responsible for about 5 to 7 % CO_2 emissions. However, during its life cycle, concrete structures are submitted to carbonation and can uptake part of CO_2 emitted during its construction (Possan *et al*., 2016). The carbonation process of concrete is principally a diffusion phenomenon. The penetration rate of carbon dioxide depends mainly on the concrete quality and the exposure condition (Liang *et al*., 2002). Carbonation is a result of CO_2 chemical reactions with alkaline products of cement hydration, in order to form calcium carbonate ($CaCO_3$) and water. This reaction ($Ca(OH)_2 + CO_2 \rightarrow CaCO_3 + H_2O$) reduces concrete pH, so, steel becomes susceptible to corrosion. On the other hand, the same reaction uptakes CO_2, since carbon dioxide that enters through concrete pore solution reacts

*Corresponding Author: Olayiwola, R. O.
Email: olayiwola.rasaq@futminna.edu.ng

with calcium hydroxide ($Ca(OH)_2$) to produce $CaCO_3$ in an opposite process to cement production ($CaCO_3 \rightarrow CaO + CO_2$). Carbonation reaction, and consequently CO2 uptake, occurs throughout concrete structure lifetime (Possan *et al*., 2016).

In order to understand and model the deterioration mechanisms and their kinetic and action in the concrete structures, countless studies have emerged in the technical and scientific community. As a result, many models to estimate carbonation depth and lifetime preview were established in recent years. These models enabled considerable advances for understanding the behavior of the exposed concrete structures over time. With the aim of estimate the carbonation depth, Possan *et al*. (2016) applied mathematical modeling to evaluate the performance of compression strength from a 20, 30 and 40 MPa concrete produced with different types of cements (CP III, CP IV and CP V, ARI) from 0 to 100 years of age. It was found out that CO_2 uptake is directly ratable to the concrete superficial area exposed to CO_2, influenced by the type of cement and concrete strength.

Tran *et al*. (2017) investigated in twelve cases of testing the effect of environment, ambient temperature and relative humidity on a concrete slab in the laboratory, to minimize the influence of wind. Their results showed that the absolute contrast between the defective and sound areas becomes more apparent with an increase of ambient temperature, and it increases at a faster rate with large and shallow delaminations than small and deep delaminations. Liang *et al*. (2002) determined the carbonation depth from the surface and at the corners of a concrete member. The carbonation depth was predicted by using a statistical method. In order to investigate the concrete carbonation problem, the three-dimensional equation of carbonation of mass, based on both the Fick first and second laws, was reduced into a one-dimensional diffusion equation of which the solution was simplified as an empirical formula. In another development, Liang and Lin (2003) described a theoretical study that is a one-dimensional linear diffusion equation with initial and boundary conditions. The mathematical model considered the relationships among unsteady state and diffusion, pore-water convective effect and chemical reaction.

In this paper, a two-dimensional mathematical model that can be used to determine the rate at which water or other substances penetrate into concrete structures is presented. Concrete is considered homogeneous, isotropic and free of crack. As a result of this, to simulate the flow analytically using eigenfunctions expansion technique, we assume the diffusion coefficient, D, of CO_2 in any direction of concrete is all the same.

2. Model Formulation

According to Miloud (2005), the permeability of concrete refers to the rate at which water or other substances (sulphates, chlorides ions, carbon dioxide, etc.), can penetrate the concrete. Following Liang and Lin (2003), the rate at which water or other substances penetrates into concrete structures can be determined using several transport mechanisms. These mechanisms often act simultaneously on the concrete structures and may include such processes as convection, diffusion, dispersion, and first-order production (Weber and DiGiano, 1996) or decay. Assume that concrete is a kind of homogeneous and isotropic material and is free of crack. This means that the diffusion coefficient, *D*, of CO_2 in any direction of concrete is all the same. The general partial differential equation that relates these factors to a two-dimensional transport process can be written as

$$\frac{\partial C}{\partial t} = D\left(\frac{\partial^2 C}{\partial x^2} + \frac{\partial^2 C}{\partial y^2}\right) - u\frac{\partial C}{\partial x} - v\frac{\partial C}{\partial y} - K_T C - r\,. \tag{1}$$

As initial and boundary conditions, we choose:

$$\left.\begin{array}{llll} C(x,y,t) = C_i; & x \geq 0, & y \geq 0, & t = 0 \\ C(x,y,t) = C_s; & x = 0, & y = 0, & t > 0 \\ C(x,y,t) = C_f; & x = L, & y = H, & t \geq 0 \end{array}\right\}, \tag{2}$$

where $C(x,y,t)$ is the concentration of substances at space *x* and y and time *t*, D_s is the diffusion coefficient, u and *v* are the pore-water velocities, K_T is the rate constant for first-order decay at a given temperature *T*, *r* is the rate constant for zero-order production, *x* is space and *t* is time, μ dynamic viscosity, k permeability, p pressure, C_i is the initial concentration of substances in concrete, C_s is the concentration of substances on the surface of concrete structure, and C_f is the concentration of substances at the interface between concrete and steel, *L* is the concrete cover thickness on the reinforcing steel.

Equation (1) consider the relationships among unsteady; $\frac{\partial C}{\partial t}$, diffusion; $D\left(\frac{\partial^2 C}{\partial x^2} + \frac{\partial^2 C}{\partial y^2}\right)$, pore-water convective effect; $\left(u\frac{\partial C}{\partial x} + v\frac{\partial C}{\partial y}\right)$, chemical reaction; $K_T C$ and rate constant for zero-order production; $-r$.

3. Method of Solution

In order to solve the concrete porosity and permeability problem modeled by Equations (1) and (2), we introduce a new space variable (Olayiwola *et al*. (2014)) as:

$$z = x + y, \tag{3}$$

then, equation (1) and the corresponding initial and boundary conditions in equation (2) becomes:

$$\frac{\partial C}{\partial t} = D_1 \frac{\partial^2 C}{\partial z^2} - U \frac{\partial C}{\partial z} - K_T C - r, \tag{4}$$

$$\left.\begin{array}{lll} C(z,\mathrm{t}) = C_i; & z \geq 0, & t = 0 \\ C(z,\tau) = C_s; & z = 0, & \tau > 0 \\ C(z,\tau) = C_f; & z = L + H = l, & \tau \geq 0 \end{array}\right\}, \tag{5}$$

where $D_1 = 2D$ and $U = (u + v)$.

Next, we assume

$$C(z,t) = e^{\alpha z + \beta t}\phi(z,t), \tag{6}$$

where α and β are the constant parameters and $\phi(z,t)$ are a new function of substances concentration. Then

$$\frac{\partial C}{\partial t} = \beta e^{\alpha z + \beta t}\phi + e^{\alpha z + \beta t}\frac{\partial \phi}{\partial t}, \tag{7}$$

$$\frac{\partial C}{\partial z} = \alpha e^{\alpha z + \beta t}\phi + e^{\alpha z + \beta t}\frac{\partial \phi}{\partial z}, \tag{8}$$

$$\frac{\partial^2 C}{\partial z^2} = \alpha^2 e^{\alpha z + \beta t}\phi + 2\alpha e^{\alpha z + \beta t}\frac{\partial \phi}{\partial z} + e^{\alpha z + \beta t}\frac{\partial^2 \phi}{\partial z^2}. \tag{9}$$

Substituting equations (6) – (9) into equation (4) gives

$$\frac{\partial \phi}{\partial t} = D_1 \frac{\partial^2 \phi}{\partial z^2} + (2\alpha D_1 - U)\frac{\partial \phi}{\partial x} + (\alpha^2 D_1 - \alpha U - K_T - \beta)\phi - \frac{r}{e^{\alpha z + \beta t}}. \tag{10}$$

In order to reduce equation (10) as a standard form of the one-dimensional diffusion equation, the coefficients of the second and third terms on the right-hand side should be equal to zero, that is:

$$2\alpha D_1 - U = 0, \tag{11}$$

$$\alpha^2 D_1 - \alpha U - K_T - \beta = 0. \tag{12}$$

From Equation (11), one has

$$\alpha = \frac{U}{2D_1}, \tag{13}$$

substituting equation (13) into equation (12), one obtains

$$\beta = -\left(\frac{U^2}{4D_1} + K_T \right). \tag{14}$$

Now the problem formulated by equations (4) and (5) changes into the control equation with initial and boundary conditions:

$$\frac{\partial \phi}{\partial t} = D_1 \frac{\partial^2 \phi}{\partial z^2} - \frac{r}{e^{\alpha z + \beta t}}, \tag{15}$$

$$\phi(z,0) = C_i e^{-\alpha z}, \qquad \phi(0,t) = C_s e^{-\beta t}, \qquad \phi(l,t) = C_f e^{-(\alpha l + \beta t)}. \tag{16}$$

3.1 Non-dimensionalisation

We non-dimensionalised equations (15) and (16) using the following set of dimensionless variables:

$$z' = \frac{z}{l}, \quad \phi' = \frac{\phi}{C_s}, \quad t' = \frac{D_1 t}{l^2}, \quad \alpha' = \alpha l, \quad \beta' = \frac{\beta l^2}{D_1}, \quad r' = \frac{r l^2}{C_s D_1} \tag{17}$$

to obtain (after dropping prime):

$$\frac{\partial \phi}{\partial t} = \frac{\partial^2 \phi}{\partial z^2} - \frac{r}{e^{\alpha z + \beta t}}, \tag{18}$$

$$\phi(z,0) = \frac{C_i}{C_s} e^{-\alpha z}, \qquad \phi(0,t) = e^{-\beta t}, \qquad \phi(1,t) = \frac{C_f}{C_s} e^{-(\alpha + \beta t)}. \tag{19}$$

3.2 Solution by Eigenfunction Expansion Method

The problem in equations (18) and (19) is non-homogeneous boundary problem. In that case, we first find a function, $\varphi(z,\tau)$ which satisfies the boundary conditions. We note that equation (20) below does the trick

$$\varphi(z,t) = e^{-\beta t} + z\left(\frac{C_f}{C_s} e^{-(\alpha + \beta t)} - e^{-\beta t} \right), \tag{20}$$

we make the change of variable:

$$\phi(z,t)=\theta(z,t)+\varphi(z,t). \tag{21}$$

Then, equations (18) and (19), respectively become:

$$\frac{\partial\theta}{\partial t}=\frac{\partial^2\theta}{\partial z^2}-\frac{r}{e^{\alpha z+\beta t}}+\beta e^{-\beta t}+\beta z\left(\frac{C_f}{C_s}e^{-(\alpha+\beta t)}-e^{-\beta t}\right), \tag{22}$$

$$\theta(z,0)=\frac{C_i}{C_s}e^{-\alpha z}-\left(1+z\left(\frac{C_f}{C_s}e^{-\alpha}-1\right)\right),\qquad \theta(0,t)=0,\qquad \theta(1,t)=0. \tag{23}$$

To solve equations (22) and (23), the solution of the form (24) below is assumed:

$$\theta(z,t)=\sum_{n=1}^{\infty}\theta_n(t)\sin\left(\frac{n\pi}{L}z\right), \tag{24}$$

where

$$\theta_n(t)=\int_0^t e^{\left(-k\left(\frac{n\pi}{L}\right)^2(t-\tau)\right)}F_n(\tau)d\tau+b_n e^{\left(-k\left(\frac{n\pi}{L}\right)^2 t\right)}, \tag{25}$$

$$F_n(t)=\frac{2}{L}\int_0^L F(z,t)\sin\left(\frac{n\pi}{L}z\right)dz, \tag{26}$$

$$b_n=\frac{2}{L}\int_0^L f(z)\sin\left(\frac{n\pi}{L}z\right)dz. \tag{27}$$

Here

$$L=1,\quad k=1,\quad F(z,t)=-\frac{r}{e^{\alpha z+\beta t}}+\beta e^{-\beta t}+\beta z\left(\frac{C_f}{C_s}e^{-(\alpha+\beta t)}-e^{-\beta t}\right),$$

$$f(z)=\frac{C_i}{C_s}e^{-\alpha z}-\left(1+z\left(\frac{C_f}{C_s}e^{-\alpha}-1\right)\right)$$

and we obtain

$$\theta(z,t)=\sum_{n=1}^{\infty}\theta_n(t)\sin(n\pi z), \tag{28}$$

where

$$\theta_n(t)=\left(\frac{2\beta\left(1-(-1)^n\right)}{n\pi}+\frac{2rn\pi\left(1+(-1)^n e^{-\alpha}\right)}{\left(\alpha^2+n^2\pi^2\right)}-\frac{2\beta(-1)^n\left(\frac{C_f}{C_s}e^{-\alpha}-1\right)}{n\pi}\right)\frac{\left(e^{-\beta t}-e^{-n^2\pi^2 t}\right)}{\left(n^2\pi^2-\beta\right)}+ \quad (29)$$

$$b_n e^{-n^2\pi^2 t}$$

and

$$b_n=\left(\frac{2\frac{C_i}{C_s}n\pi\left(1-(-1)^n e^{-\alpha}\right)}{\left(\alpha^2+n^2\pi^2\right)}+\frac{2\left((-1)^n-1\right)}{n\pi}+\frac{2(-1)^n\left(\frac{C_f}{C_s}e^{-\alpha}-1\right)}{n\pi}\right), \quad (30)$$

then

$$\phi(z,t)=\theta(z,t)+e^{-\beta t}+z\left(\frac{C_f}{C_s}e^{-(\alpha+\beta t)}-e^{-\beta t}\right). \quad (31)$$

The computations were done using computer symbolic algebraic package MAPLE.

4. Results and Discussion

We assume that a reinforced concrete structure has $C_i=0$, $C_s=1.0$, $C_f=0.2$, $U=10^{-12}$, $D=10^{-11}$, $K_T=10^{-10}$, $r=10^{-12}$, analytical solution given by equation (31) are computed using computer symbolic algebraic package MAPLE. The numerical results obtained from Eigenfunctions expansion technique are shown in Figures 1 to 8. The concentration-time relationships are displayed in Figures 1 - 4. The relation between concentration and carbonation depth are depicted in Figures 5 - 8.

Figure 1 depicts the graph of $\phi(z,t)$ against t for different values of D. It is observed that the concentration of carbon dioxide in concrete structure increases and reached steady state as time increases but decreases as diffusion coefficient increases. Figure 2 shows the graph of $\phi(z,t)$ against t at $D=10^{-11}$ and different carbonation depth z. It is observed that the concentration of carbon dioxide in concrete structure increases and reached steady state as time increases but decreases as carbonation depth increases. Figure 3 displays the graph of $\phi(z,t)$ against t at $D=10^{-12}$ and different carbonation depth z. It is observed that the concentration of carbon

dioxide in concrete structure increases and reached steady state as time increases but decreases as carbonation depth increases. Figure 4 manifests the graph of $\phi(z,t)$ against t at $D=10^{-13}$ and different carbonation depth z. It is observed that the concentration of carbon dioxide in concrete structure increases and reached steady state as time increases but decreases as carbonation depth increases.

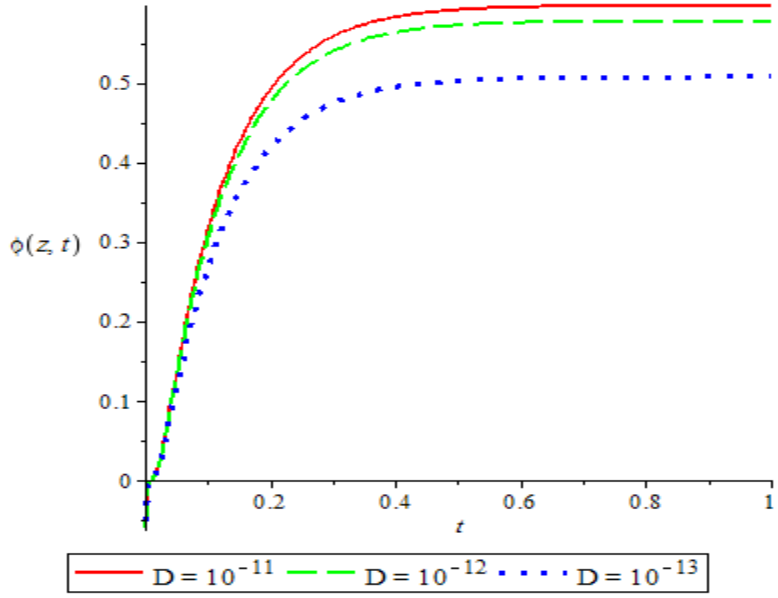

Figure 1: Concentration - time relationships for various values of D

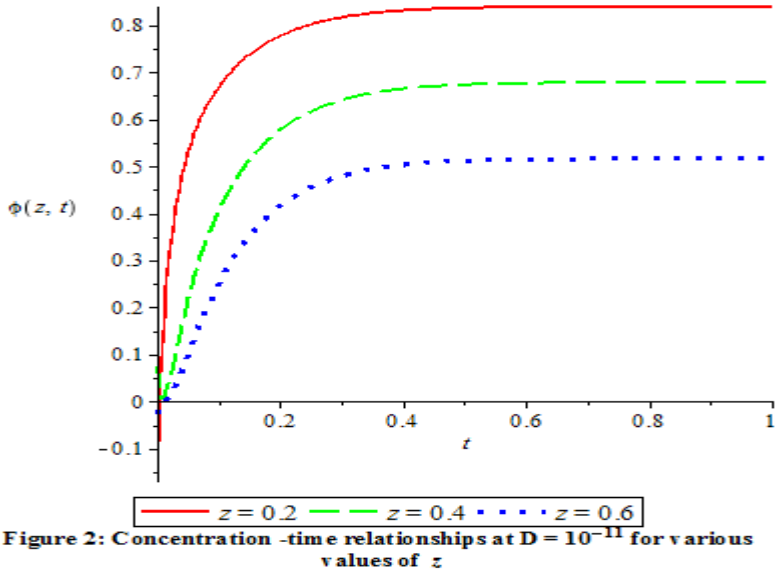

Figure 2: Concentration -time relationships at $D=10^{-11}$ for various values of z

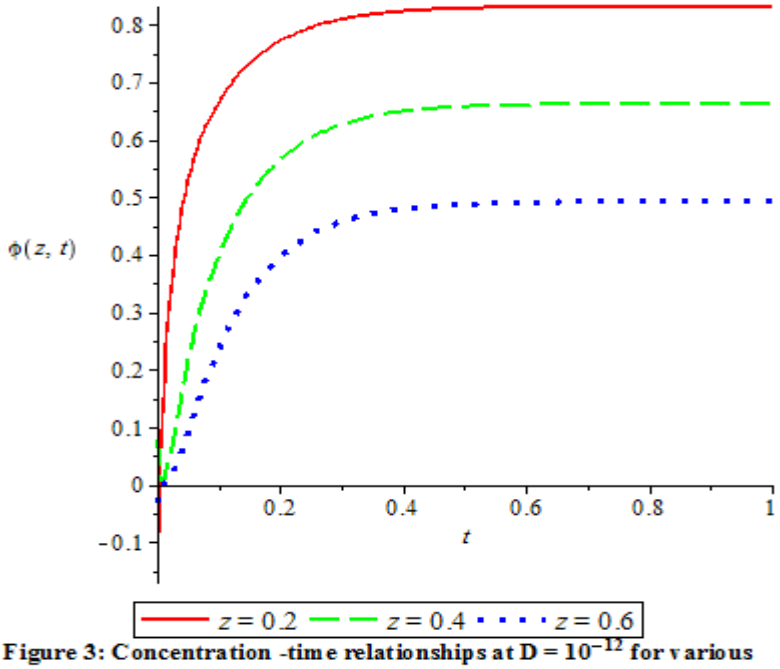

Figure 3: Concentration -time relationships at D = 10^{-12} for various values of z

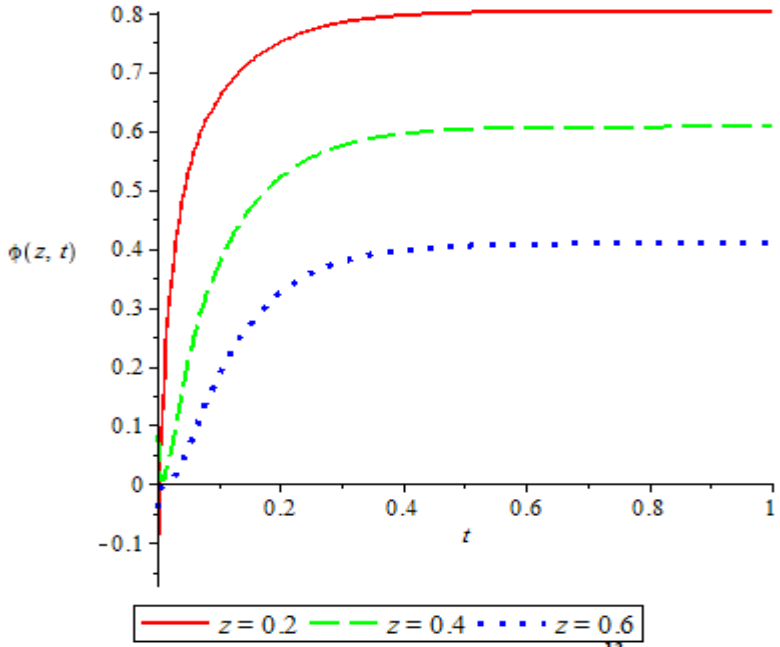

Figure 4: Concentration -time relationships at D = 10^{-13} for various values of z

Figure 5 discloses the graph of $\phi(z,t)$ against z for different values of D. It is observed that the concentration of carbon dioxide in concrete structure decreases along the carbonation depth but decreases as diffusion coefficient increases. Figure 6 shows the graph of $\phi(z,t)$ against z at $D = 10^{-11}$ and different carbonation depth z. It is observed that the concentration of carbon

dioxide in concrete structure decreases along the carbonation depth but increases as time increases. Figure 7 displays the graph of $\phi(z,t)$ against z at $D=10^{-12}$ and different carbonation depth z. It is observed that the concentration of carbon dioxide in concrete structure decreases along the carbonation depth but increases as time increases. Figure 8 depicts the graph of $\phi(z,t)$ against z at $D=10^{-13}$ and different carbonation depth z. It is observed that the concentration of carbon dioxide in concrete structure decreases along the carbonation depth but increases as time increases.

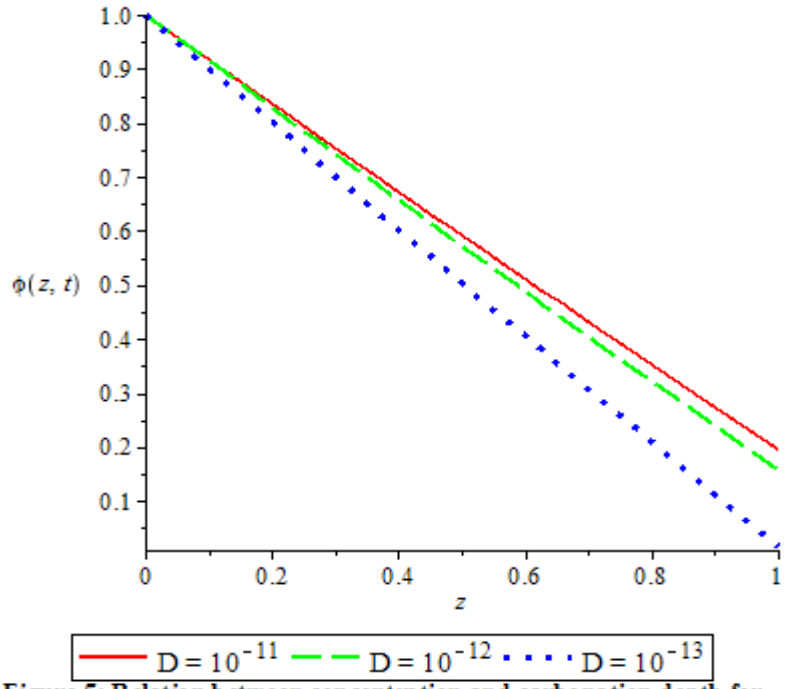

Figure 5: Relation between concentration and carbonation depth for various values of D

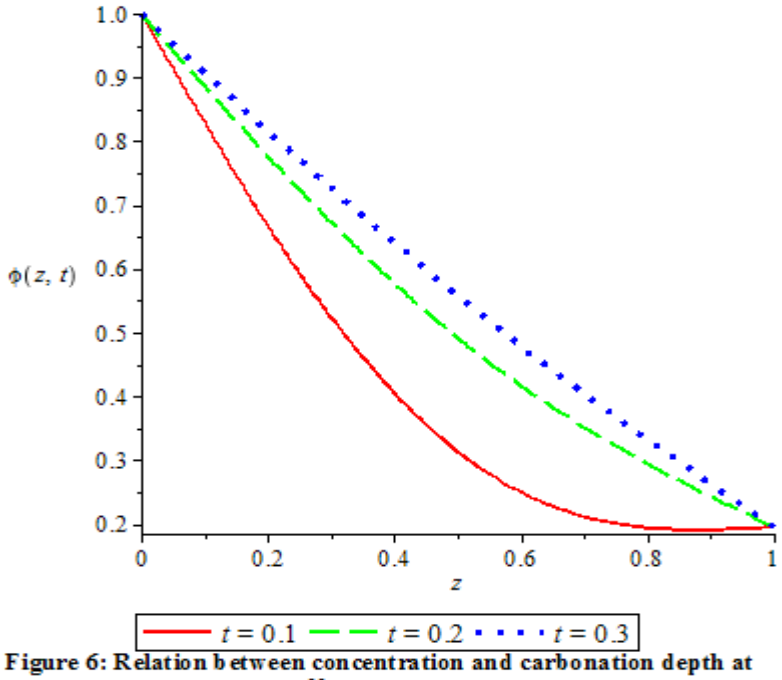

Figure 6: Relation between concentration and carbonation depth at $D = 10^{-11}$ and various time t

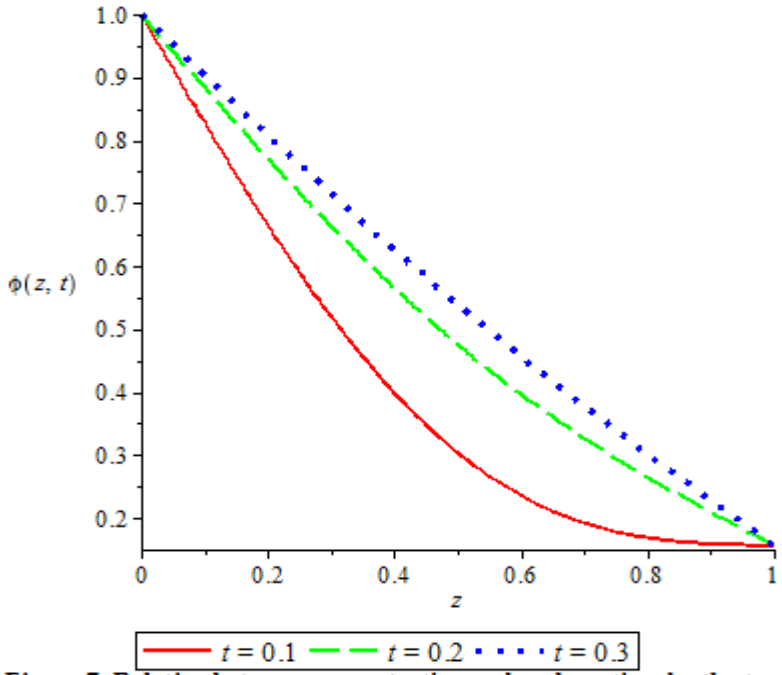

Figure 7: Relation between concentration and carbonation depth at $D = 10^{-12}$ and various time t

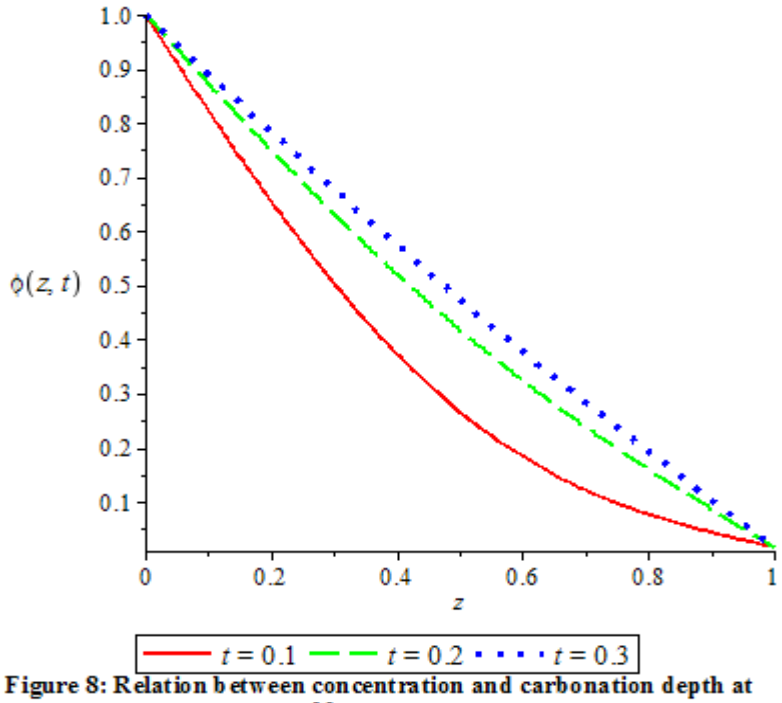

Figure 8: Relation between concentration and carbonation depth at $D = 10^{-13}$ and various time t

It is worth pointing out that the effect observed in Figures 1 to 4, is an indication that as time increases, carbon dioxide concentration in the concrete structure increases and reached steady state.

5. Conclusion

The concrete carbonation problem is one of the chemical contamination phenomena of reinforced concrete structures. A two-dimensional solute transport model incorporating rate constant for zero-order production, formulated to determine CO_2 transport in concrete is solved analytically using eigenfunctions expansion technique. The governing parameter of the problem is the diffusion coefficient (D). It is discovered that the CO_2 concentration distribution in concrete is significantly influenced by the diffusion coefficient, time and carbonation depth. The proposed mathematical model obtained from the eigenfunctions expansion technique is suitable for treating a non-uniform diffusion system with variable parameters such as the concentration, diffusion and chemical reaction of CO_2 and pore-water velocity. The results of this study may be of importance to civil engineers and scholars attempting to develop programming standards and to researchers interested in the theoretical aspects of computer programming.

References

Liang, M. T. and Lin, S. M. (2003): Mathematical modeling and Applications for Concrete Carbonation. *Journal of Marine Science and Technology*. **11** (1), 20 – 33.

Liang, M. T., Qu, W. and Liang, C. H. (2002): Mathematical Modeling and Prediction Method of Concrete Carbonation and Its Applications, *Journal of Marine Science and Technology*. **10** (2), 128 – 135.

Miloud, B. (2005): Permeability and porosity characteristics of steel fiber reinforced concrete. *Asian Journal of Civil Engineering (Building and Housing)*. **6** (4), 317-330.

Olayiwola, R. O., Bello, O. A. and Emuoyibofarhe, O. N. (2014): Mathematical Study of Contaminant Transport with Time Dependent Dispersion Coefficient and source concentration in an aquifer. *Journal of Nigerian Association of Mathematical Physics.* **28** (1), 395 – 404.

Possan, E., Felix, E. F. and Thomaz, W. A. (2016): CO2 uptake by carbonation of concrete during life cycle of building structures. *Journal of Building Pathology and Rehabilitation.* **1** (7), 1 – 9.

Tran, Q. H., Han, D., Kang, C., Haldar, A. and Huh, J. (2017): Effects of Ambient Temperature and Relative Humidity on Subsurface Defect Detection in Concrete Structures by Active Thermal Imaging. *Sensors (Basel)*. **17** (8), 1718.

Weber Jr, W. J. and DiGiano, F. A. (1996): *Process Dynamics in Environmental Systems*. John Wiley and Sons, Inc., New York, 423-502.